24th COBEM - 2017

24th ABCM International Congress of Mechanical Engineering
December 3-8, 2017, Curitiba, PR, Brazil

COBEM-2017-0378
OPTIMAL TWO-IMPULSE TRAJECTORIES FOR EARTH-MOON FLIGHT IN THE ELLIPTIC RESTRICTED THREE-BODY PROBLEM

Sandro da Silva Fernandes
Marcus Vinicius Cardoso Macêdo
Departamento de Matemática, Instituto Tecnológico de Aeronáutica, São José dos Campos – 12228-900 – SP - Brasil
sandro@ita.br; macedo.mvc@gmail.com

Luiz Arthur Gagg Filho
Departamento de Matemática, Instituto Tecnológico de Aeronáutica, São José dos Campos – 12228-900 – SP - Brasil
luizarthur.gagg@gmail.com

Abstract. *In this paper, the problem of transferring a space vehicle from a circular low Earth orbit (LEO) to a circular low Moon orbit (LMO) with minimum fuel consumption is studied. The class of two impulse trajectories is considered: a first accelerating velocity impulse tangential to the space vehicle velocity relative to Earth is applied at a circular LEO and a second braking velocity impulse tangential to the space vehicle velocity relative to Moon is applied at a circular LMO. Two dynamical models are used to describe the motion of the space vehicle: a new version of the patched-conic approximation which includes the eccentricity of the orbit of the Moon, and, the planar elliptic restricted three-body problem. In both models, the optimization problem has been solved by means of a gradient algorithm in conjunction with Newton-Raphson method. Numerical results are compared to other ones based on the classical patched-conic approximation or on the planar circular restricted three-body problem.*

Keywords: *Earth-to-Moon trajectories, optimal space trajectories, minimum fuel trajectories, elliptic model.*

1. INTRODUCTION

In this paper, the problem of transferring a space vehicle from a circular low Earth orbit (LEO) to a circular low Moon orbit (LMO) with minimum fuel consumption is considered. It is assumed that the propulsion system delivers infinite thrusts during negligible times such that the velocity changes are instantaneous, that is, the propulsion system is capable of delivering impulses. This kind of propulsion system is taken as a limit of constant ejection velocity propulsion system for highly thrust level. The class of two impulse trajectories is considered: a first accelerating velocity impulse, tangential to the space vehicle velocity relative to Earth, is applied at a circular low Earth orbit and a second braking velocity impulse, tangential to the space vehicle velocity relative to Moon, is applied at a circular low Moon orbit. The minimization of fuel consumption is equivalent to the minimization of the total characteristic velocity which is defined by the arithmetic sum of velocity changes (Marec, 1979).

The optimization problem has been formulated using an extension of the classical patched-conic approximation (Gagg Filho and da Silva Fernandes, 2015) which includes the eccentricity of the Moon orbit, and the planar elliptic restricted three-body problem (PER3BP). In the extended patched-conic approximation model, the parameters to be optimized are three: initial phase angle of space vehicle, initial position of the Moon in its orbit, and the first velocity impulse or, equivalently, the velocity of the vehicle at the insertion point in the geocentric phase. In this formulation, the time of flight and the second velocity impulse are determined from the two-body dynamics (Bate *et al*, 1971). In the PER3BP model, the parameters to be optimized are five: initial phase angle of space vehicle, time of flight, the first and the second velocity impulses, and the initial position of the Moon in its orbit. In all cases, the optimization problem has been solved using a gradient algorithm (Miele *et al*, 1969) in conjunction with Newton-Raphson method (Stoer and Bulirsch, 2002). In all models, a second optimization problem can be formulated if the initial position of the Moon is prescribed. In this way, a study about the fuel consumption parameterized by the initial position of the Moon is performed and some interesting results can be obtained. Numerical results are obtained for several final altitudes of a clockwise or counterclockwise circular low Moon orbit considering a specified altitude of a counterclockwise circular low Earth orbit. Only direct-ascent trajectories are considered in the analysis. The results are compared to other ones based on the classical patched-conic approximation or on the planar circular restricted three-body problem.

The paper is organized as follows. In Section 2, the formulation of the optimization problem based on an extended version of the patched-conic approximation is presented. The formulation of the optimization problem based on the planar elliptic three-body problem is presented in Section 3. Section 4 is dedicated to a numerical analysis of some Earth-to-Moon trajectories considering direct-ascent trajectories. General remarks are discussed in the last section.

2. OPTIMIZATION PROBLEM BASED ON PATCHED-CONIC APPROXIMATION

In this section, the optimization problem based on a new version of the patched-conic approximation, which includes the eccentricity of the orbit of the Moon, is formulated. The following assumptions are employed:

1. The Earth is fixed in space;
2. The eccentricity of the Moon orbit around Earth is considered;
3. The flight of the space vehicle takes place in the Moon orbital plane;
4. The gravitational fields of Earth and Moon are central and obey the inverse square law;
5. The trajectory has two distinct phases: geocentric and selenocentric trajectories. The geocentric phase corresponds to the portion of the trajectory which begins at the point of application of the first impulse and extends to the point of entering the Moon's sphere of influence. The selenocentric phase corresponds to the portion of trajectory in the Moon's sphere of influence and ends at the point of application of the second impulse. In each one of these phases, the space vehicle is under the gravitational attraction of only one body, Earth or Moon;
6. The class of two impulse trajectories is considered. The impulses are applied tangentially to the space vehicle velocity relative to Earth (first impulse) and Moon (second impulse).

For a given initial position of the Moon on its orbit defined by the true anomaly $f_M(t_0)$, an Earth-Moon trajectory is completely specified by four quantities: r_0 - radius of circular LEO; v_0 - velocity of the space vehicle at the point of application of the first impulse after the application of the impulse; ϕ_0 - flight path angle at the point of application of the first impulse and γ_0 - phase angle at departure. These quantities must be determined such that the space vehicle is injected into a LMO with specified altitude after the application of the second impulse. It is particularly convenient to replace γ_0 by the angle λ_1 which specifies the point at which the geocentric trajectory crosses the Moon's sphere of influence. On the other hand, it should be noted that the initial position of the Moon determines the distance *D* between Earth and Moon at the time at which the space vehicle reaches the sphere of influence of the Moon. So, it is also convenient to specify the eccentric anomaly $E_M(t_1)$, replacing the true anomaly $f_M(t_0)$, which can be determined after solving the two-point boundary value problem of going from LEO to LMO.

Equations describing each phase of an Earth-Moon trajectory are briefly presented in what follows. It is assumed that the geocentric trajectory is direct and that lunar arrival occurs prior to apoapsis of the geocentric orbit. Figure 1 shows, separately, the geometry of the geocentric phase and of the selenocentric phase for a clockwise arrival to LMO.

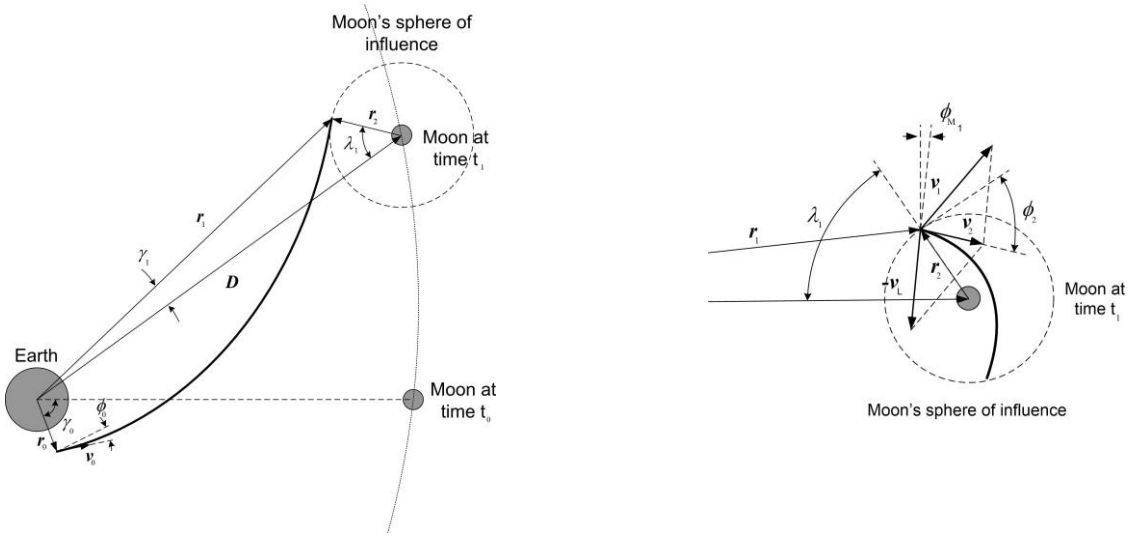

Figure 1 – Geometry of geocentric and selenocentric phases.

For a given set of initial conditions (r_0, v_0, ϕ_0) and specified eccentric anomaly $E_M(t_1)$ and angle λ_1, energy and angular momentum of the geocentric trajectory can be determined from the equations

$$\varepsilon = \frac{1}{2}v_0^2 - \frac{\mu_E}{r_0}, \tag{1}$$

$$h = r_0 v_0 \cos\phi_0, \tag{2}$$

where μ_E is Earth gravitational parameter.

From the geometry of the geocentric phase (Fig. 1), one finds

$$r_1 = \sqrt{D^2 + R_S^2 - 2DR_S \cos\lambda_1}, \tag{3}$$

$$\sin\gamma_1 = R_S \sin\lambda_1 / r_1, \tag{4}$$

where D is the distance from the Earth to the Moon at time t_1, R_S is the radius of the Moon's sphere of influence. Subscript 1 denotes quantities of the geocentric trajectory calculated at the edge of the Moon's sphere of influence.

From energy and angular momentum of the geocentric trajectory, one finds

$$v_1 = \sqrt{2\left(\varepsilon + \mu_E / r_1\right)}, \tag{5}$$

$$\cos\phi_1 = \frac{h}{r_1 v_1}. \tag{6}$$

The selenocentric phase begins at the point at which the geocentric trajectory crosses the Moon's sphere of influence. Thus,

$$r_2 = R_S, \tag{7}$$

$$\mathbf{v_2} = \mathbf{v_1} - \mathbf{v}_{M_1}, \tag{8}$$

where $\mathbf{v}_{M_1}$ is the velocity vector of the Moon relative to the center of the Earth. Subscript 2 denotes quantities of the selenocentric trajectory calculated at the edge of the Moon's sphere of influence.

From Eq. (8), one finds

$$v_2 = \sqrt{v_1^2 + v_{M_1}^2 - 2v_1 v_{M_1} \cos\left(\phi_1 - \gamma_1 - \phi_{M_1}\right)}, \tag{9}$$

$$\tan\left(\lambda_1 \pm \phi_2\right) = -\frac{v_1 \sin\left(\phi_1 - \gamma_1\right) - v_{M_1} \sin\phi_{M_1}}{v_{M_1} \cos\phi_{M_1} - v_1 \cos\left(\phi_1 - \gamma_1\right)}. \tag{10}$$

The upper sign refers to clockwise arrival to LMO and the lower sign refers to counterclockwise to LMO. ϕ_{M_1} is the flight path angle and v_{M_1} is the velocity of the Moon at time t_1, and they are computed using the well-known equations of the two-body problem (Bate *et al*, 1971).

The semi-major axis a_f and eccentricity e_f of the selenocentric trajectory are given by

$$a_f = \frac{r_2}{2 - Q_2}, \tag{11}$$

$$e_f = \sqrt{1 + Q_2\left(Q_2 - 2\right)\cos^2\phi_2}, \tag{12}$$

where $Q_2 = r_2 v_2^2 / \mu_M$ and μ_M is Moon gravitational parameter.

The second impulse is applied at the periselenium of the selenocentric trajectory such that the terminal conditions, before the impulse, are defined by

$$r_{p_M} = a_f \left(1 - e_f\right), \tag{13}$$

$$v_{p_M} = \sqrt{\frac{\mu_M \left(1 + e_f\right)}{a_f \left(1 - e_f\right)}}. \tag{14}$$

Equations (1) to (14) lead to the following two-point boundary value problem: For specified values of λ_1 and $E_M\left(t_1\right)$, and a given set of initial parameters r_0 and $\phi_0 = 0$ (the impulse is applied tangentially to the space vehicle velocity relative to Earth) determine v_0 such that the final condition $r_{p_M} = r_f$ is satisfied, r_f is the radius of LMO (both orbits, LEO and LMO, are circular). This boundary value problem can be solved by means of Newton-Raphson method (Stoer and Bulirsch, 2002).

After computing v_0, the velocity changes at each impulse can be determined

$$\Delta v_{LEO} = v_0 - \sqrt{\frac{\mu_E}{r_0}}, \tag{15}$$

$$\Delta v_{LMO} = \sqrt{\frac{\mu_M \left(1 + e_f\right)}{a_f \left(1 - e_f\right)}} - \sqrt{\frac{\mu_M}{r_f}}. \tag{16}$$

The total characteristic velocity is then given by

$$\Delta v_{Total} = \Delta v_{LEO} + \Delta v_{LMO}. \tag{17}$$

Note that the total characteristic velocity is function of λ_1 and $E_M\left(t_1\right)$ for a given set of parameters $\left(r_0, \phi_0 = 0, r_f\right)$. Accordingly, the following optimization problem can be formulated: Determine λ_1 and $E_M\left(t_1\right)$ to minimize Δv_{Total}. This minimization problem has been solved by means of a classic gradient method (Miele *et al*, 1969) in conjunction with Newton-Raphson method (Stoer and Bulirsch, 2002).

The total flight time of an Earth-Moon trajectory is given by

$$T = \Delta t_E + \Delta t_M, \tag{18}$$

where Δt_E is the flight time of the geocentric trajectory and Δt_M is the flight time of the selenocentric trajectory. These times are calculated from the well-known equations times of flight of two-body dynamics (Bate *et al*, 1971) as described in what follows:

$$\Delta t_E = \sqrt{\frac{a_0^3}{\mu_E}} \left(E_1 - e_0 \sin E_1\right), \tag{19}$$

$$\Delta t_M = \sqrt{\frac{\left(-a_f\right)^3}{\mu_M}} \left(e_f \sinh F_2 - F_2\right), \tag{20}$$

with eccentric anomaly E_1 and hyperbolic eccentric anomaly F_2 obtained from equations

$$\cos E_1 = \frac{1}{e_0}\left(1 - \frac{r_1}{a_0}\right), \qquad \cosh F_2 = \frac{1}{e_f}\left(1 - \frac{r_2}{a_f}\right). \tag{21}$$

Since lunar arrival occurs prior to apoapsis of the geocentric trajectory, $0 < E_1 \le 180°$. The semi-major axis a_0 and eccentricity e_0 of the geocentric trajectory are given by

$$a_0 = \frac{r_0}{2 - Q_0}, \qquad e_0 = \sqrt{1 + Q_0 (Q_0 - 2)\cos^2 \varphi_0}, \tag{22}$$

where $Q_0 = r_0 v_0^2 / \mu_E$. Note that each impulse is applied at the perigee of LEO and at the periselenium of LMO.

3. OPTIMIZATION PROBLEM BASED ON THE CLASSICAL VERSION OF PCR3BP

In this section, the optimization problem based on PER3BP is formulated. The following assumptions are employed:

1. Earth and Moon move around the center of mass of the Earth-Moon system.;
2. The eccentricity of the Moon orbit around Earth is considered;
3. The flight of the space vehicle takes place in the Moon orbital plane;
4. The space vehicle is subject to only the gravitational fields of Earth and Moon;
5. The gravitational fields of Earth and Moon are central and obey the inverse square law;
6. The class of two impulse trajectories is considered. The impulses are applied tangentially to the space vehicle velocity relative to Earth (first impulse) and Moon (second impulse).

Consider an inertial reference frame G*xy* contained in the Moon orbital plane: its origin is the center of mass G of the Earth-Moon system; the *x*-axis points towards the Moon position at the initial time $t_0 = 0$ and the *y*-axis is perpendicular to the *x*-axis.

In the G*xy* reference frame, the motion of the space vehicle (P) is described by the following differential equations:

$$\frac{dx_P}{dt} = u_P$$

$$\frac{dy_P}{dt} = v_P$$

$$\frac{du_P}{dt} = -\frac{\mu_E}{r_{EP}^3}(x_P - x_E) - \frac{\mu_M}{r_{MP}^3}(x_P - x_M)$$

$$\frac{dv_P}{dt} = -\frac{\mu_E}{r_{EP}^3}(y_P - y_E) - \frac{\mu_M}{r_{MP}^3}(y_P - y_M), \tag{23}$$

where r_{PE} and r_{PM} are, respectively, the radial distances of space vehicle from Earth (E) and Moon (M), that is, $r_{EP}^2 = (x_P - x_E)^2 + (y_P - y_E)^2$ and $r_{MP}^2 = (x_P - x_M)^2 + (y_P - y_M)^2$. Because the origin of the inertial reference frame G*xy* is the center of mass of Earth-Moon system, the position vectors of the Earth and the Moon are, respectively, defined by $\boldsymbol{r}_E = (x_E, y_E)$ and $\boldsymbol{r}_M = (x_M, y_M)$. Since the Moon orbit around Earth is defined by an ellipse, the Earth and Moon inertial coordinates are given by well-known equations from the solution of the two-body problem

$$x_E(t) = -\mu x_M(t) \qquad y_E(t) = -\mu y_M(t)$$

$$x_M(t) = r_M \cos(\omega_M + f_M) \qquad y_M(t) = r_M \sin(\omega_M + f_M), \tag{24}$$

where $\mu = \mu_M / \mu_E$, ω_M is the argument of periapsis of the Moon's orbit, measured from the *x*-axis of the inertial reference frame G*xy*, f_M is the true anomaly and r_M is the distance from Earth to Moon at time *t* and it is given by the polar equation of a conic section (Bate et al, 1971)

$$r_M = \frac{a_M (1 - e_M^2)}{1 + e_M \cos f_M}, \tag{25}$$

where a_M is the semi-major axis and e_M is the eccentricity of the Moon's orbit.

The initial conditions of the system of differential equations correspond to the position and velocity vectors of the space vehicle after the application of the first impulse. The initial conditions ($t_0 = 0$) can be written as follows:

$$x_P(0) = x_{EP}(0) + x_E(0) = r_{EP}(0)\cos\theta_{EP}(0) + x_E(0), \tag{26}$$

$$y_P(0) = y_{EP}(0) + y_E(0) = r_{EP}(0)\sin\theta_{EP}(0) + y_E(0), \tag{27}$$

$$u_P(0) = u_{EP}(0) + u_E(0) = -\left[\sqrt{\frac{\mu_E}{r_{EP}(0)}} + \Delta v_{LEO}\right]\sin\theta_{EP}(0) + u_E(0), \tag{28}$$

$$v_P(0) = v_{EP}(0) + v_E(0) = \left[\sqrt{\frac{\mu_E}{r_{EP}(0)}} + \Delta v_{LEO}\right]\cos\theta_{EP}(0) + v_E(0), \tag{29}$$

where Δv_{LEO} is the velocity change at the first impulse, $r_{EP}(0) = r_{EP_0}$ and $\theta_{EP}(t)$ is the angle defining the position of the space vehicle in the inertial reference frame G*xy* at time *t*, more precisely the angle which the position vector $\boldsymbol{r}_P$ forms with *x*-axis. It should be noted that $\mathbf{r}_{EP}(0)$ and $\mathbf{v}_{EP}(0)$ are orthogonal, because the impulse is applied tangentially to LEO, assumed circular. The components of the position vector and of the velocity vector of the Earth at time $t_0 = 0$ are obtained straightforwardly from Eqs (24) and (25). Note that the true anomaly $f_M(t_0)$ defining the initial position of the Moon must be specified.

The final conditions of the system of differential equations correspond to the position and velocity vectors of the space vehicle before the application of the second impulse. The final conditions ($t_f = T$) can be written as follows:

$$x_P(T) = x_{MP}(T) + x_M(T) = r_{MP}(T)\cos\theta_{MP}(T) + x_M(T), \tag{30}$$

$$y_P(T) = y_{MP}(T) + y_M(T) = r_{MP}(T)\sin\theta_{MP}(T) + y_M(T), \tag{31}$$

$$u_P(T) = u_{MP}(T) + u_M(T) = \pm\left[\sqrt{\frac{\mu_M}{r_{MP}(T)}} + \Delta v_{LMO}\right]\sin\theta_{MP}(T) + u_M(T), \tag{32}$$

$$v_P(T) = v_{MP}(T) + v_M(T) = \mp\left[\sqrt{\frac{\mu_M}{r_{MP}(T)}} + \Delta v_{LMO}\right]\cos\theta_{MP}(T) + v_M(T), \tag{33}$$

where Δv_{LMO} is the velocity change at the second impulse, $r_{MP}(T) = r_{MP_f}$ and $\theta_{MP}(t)$ is the angle which the position vector $\mathbf{r}_{MP}$ forms with *x*-axis. The upper sign refers to clockwise arrival to LMO and the lower sign refers to counterclockwise to LMO. The components of the position vector and of the velocity vector of the Moon at time *T* are obtained straightforwardly from Eqs (24) and (25).

The angle $\theta_{MP}(T)$ is free and can be eliminated. After the problem has been solved, the angle $\theta_{MP}(T)$ can be calculated from Eqs (30) and (31). So, combining Eqs (30) – (33), the final conditions can be put in the form:

$$\left(x_P(T) - x_M(T)\right)^2 + \left(y_P(T) - y_M(T)\right)^2 = \left(r_{MP}(T)\right)^2, \tag{34}$$

$$\left(u_P(T) - u_M(T)\right)^2 + \left(v_P(T) - v_M(T)\right)^2 = \left[\sqrt{\frac{\mu_M}{r_{MP}(T)}} + \Delta v_{LMO}\right]^2, \tag{35}$$

$$\left(x_P(T) - x_M(T)\right)\left(v_P(T) - v_M(T)\right) - \left(y_P(T) - y_M(T)\right)\left(u_P(T) - u_M(T)\right) = \mp r_{PM}(T)\left[\sqrt{\frac{\mu_M}{r_{MP}(T)}} + \Delta v_{LMO}\right]. \tag{36}$$

The upper sign refers to clockwise arrival to LMO and the lower sign refers to counterclockwise to LMO. It should be noted that the constraint defined by Eq. (33) is derived from the angular momentum considering a direct (counterclockwise arrival) or a retrograde (clockwise arrival) orbit around the Moon.

4. RESULTS

In this section, results are presented for lunar missions using the two dynamical models previously described and are compared to the results obtained considering the optimization problems based on the classical patched-conic approximation or on the planar circular restricted three-body problem. The following data are used:

$\mu_E = 3.986 \times 10^5$ km^3/s^2, $\mu_M = 4.903 \times 10^3$ km^3/s^2,
$D = 384400$ km (distance from the Earth to the Moon),
a_E = 6378 km (Earth radius), $a_M = 1738$ km (Moon radius),
h_0 = 167 km (altitude of LEO), $h_f = 100,\ 200,\ 300,\ 400,\ 500$ km (altitude of LMO).

The algorithm based on gradient algorithm in conjunction with Newton-Raphson method, described in this paper, uses a Runge-Kutta-Fehlberg method of order 4 and 5, with step-size control, and, relative error tolerance of 10^{-10} and absolute error tolerance of 10^{-11} (Forsythe *et al*, 1977), and, the terminal constraints are satisfied with an error lesser than 10^{-8}. In all simulations, canonical units are used: 1 distance unit = a_E and 1 time unit = $\sqrt{a_e^3/\mu_E}$, such that $\mu_E = 1.0$ d.u.^{3}/t.u.^{2}

Table 1 shows the results for lunar missions with clockwise arrival at LMO and Table 2 shows the results for lunar missions with counterclockwise arrival at LMO. The departure from LEO is counterclockwise for all missions. The major parameters that are presented in these tables are the velocity changes Δv_{LEO} and Δv_{LMO} at each impulse, the total characteristic velocity $\Delta v_{Total} = \Delta v_{LEO} + \Delta v_{LMO}$, the flight time of lunar mission *T*, the initial position of the space vehicle in the inertial reference frame G*xy* at the initial time $t_0 = 0$ defined by the angle $\theta_{EP}(0)$, and, the initial position of the Moon defined by the true anomaly $f_M(0)$.

Results in Tabs. 1 and 2 show the good agreement between the results of the elliptic patched-conic approximation and the elliptic three-body problem. There exists a small difference between the total velocity increments of these models. This difference occurs mainly to the second velocity increment: for a LMO altitude of 100 km with clockwise arrival, for instance, the difference between the increments Δv_{LMO} is 29 m/s with the elliptic patched-conic approximation presenting the smaller increment. The same pattern is noted when the classical patched-conic approximation is compared to the classical three-body problem. An important fact highlighted by Tabs. 1 and 2 is that both elliptic models, patched-conic approximation and three-body problem, waste less fuel consumption than the classical models: for a clockwise arrival at 100 km altitude in the LMO, the elliptic patched-conic approximation has a total velocity increment 9 m/s less than that of the classical patched-conic approximation, and, the elliptic three-body model has a total velocity increment 10 m/s less than that of the classical three-body model. This same behavior is noticed for the others LMO altitude and with counterclockwise arrival. Despite these differences be small, the saving of fuel consumption in elliptic models can be considerable for trajectories with larger times of flight. Moreover, one must choose carefully the initial position of the Moon for the elliptic three-body model or the position defined by the eccentric anomaly $E_M(t_1)$ for the elliptic patched-conic approximation in order to determine the optimal trajectory that saves more fuel. Note that the classical models do not present results for the initial position of the Moon since its orbit is circular. Also, the proposed elliptic models exhibit a robustness to converge the results by means of the Newton-Raphson method since several altitudes of LMO are utilized.

Table 1 – Lunar mission, clockwise LMO arrival, major parameters. LEO orbit = 167 km.

LMO altitude *km*	***Model***	Δv_{Total} *km/s*	Δv_{LEO} *km/s*	Δv_{LMO} *km/s*	T *days*	$\theta_{EP}(0)$ *deg*	$f_M(0)$ *deg*
100	*Patched-conic*	3.926855	3.140943	0.785913	4.944	−113.628	–
	Elliptic patched-conic	3.917459	3.145649	0.771809	5.338	−113.997	112.987
	classical PCR3BP	3.956983	3.141269	0.815714	4.770	−113.776	–
	PER3BP	3.946462	3.145610	0.800851	5.131	−114.271	113.943
200	*Patched-conic*	3.912036	3.140981	0.771055	4.948	−113.596	–
	Elliptic patched-conic	3.902288	3.145686	0.756602	5.342	−113.965	112.982
	classical PCR3BP	3.942884	3.141308	0.801576	4.771	−113.760	–
	PER3BP	3.931981	3.145622	0.786359	5.132	−114.137	112.003
300	*Patched-conic*	3.898453	3.141019	0.757434	4.951	−113.565	–
	Elliptic patched-conic	3.888366	3.145721	0.742644	5.346	−113.934	112.981
	Classical PCR3BP	3.929999	3.141347	0.788651	4.779	−113.682	–
	PER3BP	3.918745	3.145658	0.773087	5.137	−114.099	112.003
400	*Patched-conic*	3.885958	3.141056	0.744902	4.955	−113.534	–
	Elliptic patched-conic	3.875540	3.145756	0.729784	5.350	−113.903	112.955
	classical PCR3BP	3.918177	3.141385	0.776791	4.780	−113.674	–
	PER3BP	3.906585	3.145694	0.760891	5.141	−114.062	112.002
500	*Patched-conic*	3.874423	3.141093	0.733330	4.958	−113.504	–
	Elliptic patched-conic	3.863684	3.145790	0.717894	5.353	−113.874	112.960
	classical PCR3BP	3.907296	3.141423	0.765873	4.788	−113.596	–
	PER3BP	3.895376	3.145729	0.749647	5.145	−114.026	112.003

Table 2 – Lunar mission, counterclockwise LMO arrival, major parameters

LMO altitude *km*	***Model***	Δv_{Total} *km/s*	Δv_{LEO} *km/s*	Δv_{LMO} *km/s*	T *days*	$\theta_{EP}(0)$ *deg*	$f_M(0)$ *deg*
100	*Patched-conic*	3.922364	3.138214	0.784150	4.793	–115.762	–
	Elliptic patched-conic	3.913337	3.143048	0.770289	5.128	–116.376	110.932
	classical PCR3BP	3.951898	3.138546	0.813352	4.572	–116.466	–
	PER3BP	3.941740	3.143058	0.798682	4.925	–117.058	117.796
200	*Patched-conic*	3.907369	3.138173	0.769196	4.792	–115.789	–
	Elliptic patched-conic	3.898006	3.143009	0.754997	5.128	–116.397	110.939
	classical PCR3BP	3.937589	3.138504	0.799086	4.574	–116.456	–
	PER3BP	3.927048	3.142984	0.784064	4.919	–116.958	114.990
300	*Patched-conic*	3.893613	3.138133	0.755480	4.792	–115.816	–
	Elliptic patched-conic	3.883925	3.142972	0.740953	5.128	–116.420	110.964
	classical PCR3BP	3.924494	3.138462	0.786032	4.571	–116.511	–
	PER3BP	3.913619	3.142944	0.770675	4.917	–116.997	114.996
400	*Patched-conic*	3.880944	3.138093	0.742851	4.791	–115.843	–
	Elliptic patched-conic	3.870942	3.142935	0.728008	5.128	–116.440	110.950
	classical PCR3BP	3.912465	3.138422	0.774044	4.568	–116.563	–
	PER3BP	3.901267	3.142906	0.758360	4.915	–117.035	114.997
500	*Patched-conic*	3.869238	3.138054	0.731184	4.791	–115.869	–
	Elliptic patched-conic	3.858931	3.142898	0.716033	5.128	–116.462	110.951
	classical PCR3BP	3.901377	3.138382	0.762995	4.566	–116.612	–
	PER3BP	3.889866	3.142868	0.746997	4.913	–117.072	114.997

Finally, note that:

1. Lunar missions with clockwise LMO arrival spend more fuel than lunar missions with counterclockwise LMO arrival for both elliptic and classical models;
2. Despite the flight time be nearly the same for all lunar missions with clockwise LMO arrival and for lunar missions with counterclockwise LMO arrival, the elliptic models present a time of flight larger than the classical models: for a clockwise arrival at a LMO with 100 km altitude, the elliptic patched-conic approximation presents a time of flight 0.335 days larger than the classical patched-conic approximation.
3. The second change velocity Δv_{LMO} decreases with the LMO altitude for elliptic and classical models.
4. Elliptic and classical models present the flight time with clockwise LMO arrival larger than the flight time for lunar missions with counterclockwise LMO arrival.
5. The optimal initial phase angle $\theta_{EP}(0)$ of the space vehicle and the optimal initial position of the Moon $f_M(0)$ change with the LMO altitude: for clockwise arrival, the increase of the LMO altitude decreases slightly $f_M(0)$ and decreases slightly the magnitude of $\theta_{EP}(0)$; for counterclockwise arrival, the increase of the LMO altitude increases slightly $f_M(0)$ and increases slightly the magnitude of $\theta_{EP}(0)$.

Some of the general results of the classical models are quite similar to the ones described by Miele and Mancuso (2001) and Gagg Filho and da Silva Fernandes, 2015.

5. CONCLUSION

This paper formulates Earth-Moon trajectories based on a new approach of the lunar patched-conic approximation that includes the eccentricity of the Moon's orbit around Earth. The Earth-Moon trajectory is also formulated based on the elliptic restricted three-body problem. In order to determine the optimal trajectories, optimization problems are solved in both models by means of a gradient algorithm in conjunction with Newton-Raphson method. The optimal results of both elliptic models are compared to the results based on the classical patched-conic approximation and based on the circular restricted three-body problem. The results show that both elliptic models, patched-conic approximation and three-body problem, waste less fuel consumption than the classical models. Despite these differences be small, the saving of fuel consumption in elliptic models can be considerable for trajectories with larger times of flight. This fact will be investigated in future works. Moreover, one must choose carefully the initial position of the Moon for the elliptic three-body model or the position defined by the eccentric anomaly $E_M(t_1)$ for the elliptic patched-conic approximation in order to determine the optimal that saves more fuel.

6. ACKNOWLEDGEMENTS

This research has been supported by CAPES, by CNPq under contract 304913/2013-8 and supported by grant 2008/56241-8 and 2012/25308-5, São Paulo Research Foundation (FAPESP).

7. REFERENCES

Bate, R.R., Mueller, D.D. and White, J.E., 1971. *Fundamentals of astrodynamics*. Courier Dover Publications, New York.

Forsythe, G.E., Malcolm, M.A. and Moler, C.B., 1977. *Computer methods for mathematical computations*, Vol. 8. Prentice-Hall, Englewood Cliffs, New Jersey, USA.

Gagg Filho, L.A. and da Silva Fernandes, S., 2015. "Optimal round trip lunar missions based on the patched-conic approximation". *Computational and Applied Mathematics*, pp. 1–35.

Marec, J.P., 1979. *Optimal space trajectories*. Elsevier, New York, NY.

Miele, A., Huang, H.Y. and Heideman, J.C., 1969. "Sequential gradient-restoration algorithm for the minimization of constrained functions–ordinary and conjugate gradient versions". *Journal of Optimization Theory and Applications*, Vol. 4, No. 4, pp. 213–243.

Miele, A. and Mancuso, S., 2001. "Optimal trajectories for earth-moon-earth flight". Acta Astronautica, Vol. 49, No. 2, pp. 59–71.

Stoer, J. and Bulirsch, R., 2002. *Introduction to Numerical Analysis*. Springer-Verlag, New York, 3rd edition.

8. RESPONSIBILITY NOTICE

The authors are the only responsible for the printed material included in this paper.